ELSEVIER

Journal of Organometallic Chemistry 555 (1998) 25–33

Journal of Organometallic Chemistry

Mixed-metal cluster chemistry VIII[1]: phosphite substitution at $[CpWIr_3(CO)_{11}]$; X-ray crystal structure of $[CpWIr_3(\mu\text{-}CO)_3(CO)_6\{P(OPh)_3\}_2]$

Susan M. Waterman [a], Mark G. Humphrey [a,*], David C.R. Hockless [b]

[a] *Department of Chemistry, Australian National University, Canberra, ACT 0200, Australia*

[b] *Research School of Chemistry, Australian National University, Canberra, ACT 0200, Australia*

Received 20 August 1997

Abstract

Reactions of $[CpWIr_3(CO)_{11}]$ (**1**) with stoichiometric amounts of phosphites afford the substitution products $[CpWIr_3(\mu\text{-}CO)_3(CO)_{8\text{-}n}(L)_n]$ [L = $P(OMe)_3$, $n = 1$ (**2**), 2 (**3**), 3 (**4**); L = $P(OPh)_3$, $n = 1$ (**5**), 2 (**6**), 3 (**7**)] in fair to excellent yields (29–71%). Clusters **2**, **4**, **5** and **7** are fluxional in solution, with the interconverting isomers resolvable at low temperatures. A structural study of **6** reveals that the three edges of a WIr_2 face of the tetrahedral core are spanned by bridging carbonyls, and that iridium-bound triphenylphosphites ligate radially and axially and the tungsten-bound cyclopentadienyl coordinates axially with respect to this WIr_2 face. Information from this crystal structure, ^{31}P-NMR data, and results with analogous triphenylphosphine-ligated tungsten–triiridium clusters have been employed to suggest coordination geometries for the isomers.

Keywords: Tungsten; Iridium; Carbonyl; Cyclopentadienyl; Cluster; Phosphite; Crystal structure

1. Introduction

Mixed-metal clusters continue to attract significant interest [2–6], due in some part to the belief that the polar M–M′ bonds resulting from the combination of differing metals may induce enhanced or novel forms of substrate activation compared to that observed with homometallic clusters. A second important factor which has been probed in a number of recent studies is the possibility for metalloselectivity of a reagent, with most work utilizing phosphines, amongst the most fundamental reagents in organotransition metal chemistry [2,7–25]. The vast majority of these studies have involved mixed-metal clusters incorporating metals from the same group or adjacent groups. However, it seems logical that the use of clusters incorporating widely-differing metals should be probed to maximize the possibility of substrate activation or metalloselectivity. With this in mind, we have been investigating the chemistry of the 'very mixed' group 6–9 tetrahedral clusters $[Cp_xM_xIr_{4-x}(CO)_{12-x}]$ (M = Mo, W; $x = 1, 2$), assessing the significance of the heterometallic core by benchmarking results against those of the 'parent' cluster $[Ir_4(CO)_{12}]$ ($x = 0$) [1,26–31]. A particular focus of our studies has been to understand the ligand substitution chemistry and, to this end, we have investigated the reactivity of $[CpMIr_3(CO)_{11}]$ towards phosphines [26,27,31]. Replacement of carbonyl by phosphine results in the carbonyl ligand geometry in the ground state of both the homometallic and heterometallic systems shifting from all-terminal to one in which the three edges of one face of the tetrahedral core are spanned by bridging carbonyls, giving three different ligation sites with respect to this $M_3(\mu\text{-}CO)_3$ plane, namely radial, axial and apical (Fig. 1). The heterometallic system is

---

* Corresponding author. Tel.: +61 2 62492927; fax: +61 2 62490760; e-mail: Mark.Humphrey@anu.edu.au

0022-328X/98/$19.00 © 1998 Elsevier Science S.A. All rights reserved.
PII S0022-328X(97)00686-4

potentially more complex than the homometallic, as the group 6 metal may be apical or basal and, for the latter, the cyclopentadienyl ligand may be radial or axial. The presence of the cyclopentadienyl ligand also results in the heterometallic clusters being effectively monosubstituted; the most appropriate comparison of coordination geometries upon substitution is thus between $[CpMIr_3(CO)_{11-n}(L)_n]$ and $[Ir_4(CO)_{12-(n+1)}(L)_{(n+1)}]$.

Although the least sterically hindered sites are the radial sites (Fig. 1), most monosubstituted clusters have ligands in an axial site, presumably an electronic effect [16]. Homometallic cluster substitution then proceeds at a different basal metal to afford bis-substituted derivatives with radial, axial coordination for large ligands or diaxial coordination for small ligands. In contrast, the clusters $[CpWIr_3(\mu\text{-}CO)_3(CO)_7(PPh_3)]$ and $[CpWIr_3(\mu\text{-}CO)_3(CO)_7(PMe_3)]$ exhibit radial, axial and/or axial, apical geometries [27]. The third incoming ligand occupies a basal coordination site to minimize steric effects, to give diradial, axial derivatives (most common) or radial, diaxial derivatives. In most cases the fourth ligand substitutes at the apical metal, forcing two ligands on the $M_{apical}(M_{basal})_2$ face into axial sites and the remaining ligand into a radial site. In addition to the crystallographically confirmed geometries, other isomers frequently exist in equilibrium in solution, with interconversion resulting from ligand (usually CO) scrambling. Studies of ligand fluxionality on clusters have been summarized [32–35].

In addition to the extensive studies of phosphine substitution at tetrairidium clusters [36–52], phosphite substitution has also been of interest. The phosphite ligand in $[Ir_4(CO)_{11}\{P(OPh)_3\}]$ [39] is proposed to be axially ligated on the basis of IR spectroscopy, whereas the tripodal phosphite $P(OCH_2)_3CEt$ affords a structurally characterized mono-substituted derivative with an all-terminal carbonyl geometry [53]. Detailed studies have revealed that these mono-substituted derivatives consist of three interconverting isomers in solution possessing the all-terminal ligand geometry or an edge-bridged structure with the phosphite ligand occupying radial or axial sites, which correspond to three minima on the kinetic pathway of CO scrambling, and whose relative energies vary independently within a small range (1–9 kJ mol^{-1} at 298 K) [53]. Darensbourg and co-workers have obtained $[Ir_4(CO)_8\{P(OMe)_3\}_4]$ and have suggested that it adopts an unusual triaxial, apical geometry [42]. These reports in the tetrairidium system prompted us to extend our tungsten–iridium studies to embrace phosphites, and we report herein the reactivity of **1** toward one, two or three equivalents of $P(OMe)_3$ or $P(OPh)_3$, the characterization by a single-crystal X-ray study of the bis-triphenylphosphite derivative, and the suggested coordination geometries of all other derivatives.

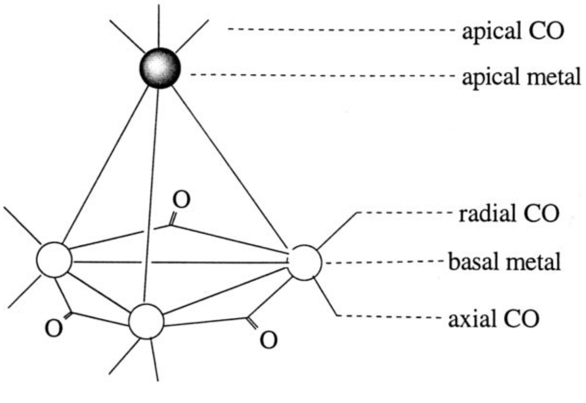

Fig. 1.

2. Results and discussion

2.1. Syntheses and characterization

The reactions of $[CpWIr_3(CO)_{11}]$ (**1**) with *n* equivalents of $P(OMe)_3$ or $P(OPh)_3$ ($n = 1$ or 2) proceed in dichloromethane at room temperature to afford the clusters $[CpWIr_3(\mu\text{-}CO)_3(CO)_{8-n}\{P(OMe)_3\}_n]$ [$n = 1$ (**2**) or $n = 2$ (**3**)] or $[CpWIr_3(\mu\text{-}CO)_3(CO)_{8-n}\{P(OPh)_3\}_n]$ [$n = 1$ (**5**) or $n = 2$ (**6**)], respectively, as the major or sole reaction products in good yields (41–71%). Although low yields are obtained upon reaction of **1** with three equivalents of the phosphites at room temperature, better yields of $[CpWIr_3(\mu\text{-}CO)_3(CO)_5\{P(OMe)_3\}_3]$ (**4**) and $[CpWIr_3(\mu\text{-}CO)_3(CO)_5\{P(OPh)_3\}_3]$ (**7**) are obtained by heating **1** with a slight excess of the appropriate phosphite in refluxing dichloromethane for 3 h. The clusters **2**–**7** have been characterized by a combination of IR, ^{1}H-, ^{13}C- and ^{31}P-NMR spectroscopies, mass spectrometry and satisfactory microanalyses. Infrared spectra suggest the presence of edge-bridging carbonyl ligands in all complexes [υ(CO) 1801–1854 cm^{-1}], which contrasts with the all-terminal geometry of the precursor **1**, but is similar to that seen for analogous triphenylphosphine and trimethylphosphine derivatives [27]; the number of bands in the terminal carbonyl ligand υ(CO) region is indicative of the presence of isomers. The ^{1}H-NMR spectra contain signals assigned to cyclopentadienyl and methoxy groups for **2**, **3** and **4**, and cyclopentadienyl and phenoxy groups for **5**, **6** and **7**, in the appropriate ratios. The mass spectra of complexes **2** and **5** contain molecular ions, and all spectra contain fragment ions corresponding to stepwise loss of carbonyls; isotope patterns are consistent with the presence of three iridium atoms and one tungsten atom.

Table 1
Crystallographic data for **6**

Formula	$C_{50}H_{35}Ir_3O_{15}P_2W$
Formula weight	1698.28
Space group	$P2_1/n$ (no. 14)
Crystal system	Monoclinic
a (Å)	16.560(3)
b (Å)	12.712(4)
c (Å)	24.522(2)
β (deg)	105.139(9)
V (Å^3)	4983(2)
ρ_{calc} (g cm^{-3})	2.26
Z	4
μ (mm^{-1})	10.4
Specimen size (mm^3)	0.48 × 0.24 × 0.16
A* (min, max)	0.39, 1.00
$2\Theta_{max}$ (deg)	50.1
N	9246
N_o	6076
R	0.037
R_w	0.027

2.2. X-ray structural study of [CpWIr$_3$(μ-CO)$_3$(CO)$_6${P(OPh)$_3$}$_2$] (6)

The molecular structure of **6** as determined by a single-crystal X-ray study is consistent with the formulation given above, defines the substitution sites of the phosphites, and aids interpretation of the ^{31}P-NMR spectra (see below). A summary of crystal and refinement data is found in Table 1, and selected bond distances and angles are listed in Table 2. An ORTEP plot showing the molecular geometry and atomic numbering scheme is shown in Fig. 2.

Table 2
Important bond lengths and angles for **6**

Ir(1)–Ir(2)	2.6941(5)	Ir(1)–Ir(3)	2.7281(6)
Ir(2)–Ir(3)	2.7125(6)	Ir(1)–W(1)	2.8042(6)
Ir(2)–W(1)	2.8485(5)	Ir(3)–W(1)	2.8990(8)
Ir(1)–P(1)	2.230(3)	Ir(2)–P(2)	2.239(3)
Ir(1)–C(1)	2.048(9)	Ir(1)–C(11)	1.830(9)
Ir(1)–C(48)	2.080(8)	Ir(2)–C(1)	2.139(9)
Ir(2)–C(2)	2.157(9)	Ir(2)–C(22)	1.89(1)
Ir(3)–C(31)	1.89(1)	Ir(3)–C(32)	1.909(9)
Ir(3)–C(33)	1.918(9)	W(1)–C(01)	2.276(9)
W(1)–C(02)	2.30(1)	W(1)–C(03)	2.33(1)
W(1)–C(04)	2.29(1)	W(1)–C(05)	2.282(9)
W(1)–C(2)	2.134(9)	W(1)–C(3)	1.978(9)
W(1)–C(48)	2.146(9)		
Ir(2)–Ir(1)–Ir(3)	60.03(1)	Ir(2)–Ir(1)–W(1)	62.37(1)
Ir(3)–Ir(1)–W(1)	63.19(2)	Ir(3)–Ir(2)–W(1)	62.79(2)
Ir(1)–Ir(2)–Ir(3)	60.61(1)	Ir(1)–Ir(2)–W(1)	60.71(1)
Ir(1)–Ir(3)–Ir(2)	59.36(1)	Ir(1)–Ir(3)–W(1)	59.69(1)
Ir(2)–Ir(3)–W(1)	60.90(2)	Ir(1)–W(1)–Ir(2)	56.92(1)
Ir(1)–W(1)–Ir(3)	57.12(1)	Ir(2)–W(1)–Ir(3)	56.31(1)
Ir(2)–Ir(1)–P(1)	139.12(7)	Ir(3)–Ir(1)–P(1)	100.44(7)
W(1)–Ir(1)–P(1)	144.54(7)	Ir(1)–Ir(2)–P(2)	109.38(8)
Ir(3)–Ir(2)–P(2)	167.18(7)	W(1)–Ir(2)–P(2)	105.90(7)

Complex **6** has the WIr_3 pseudotetrahedral framework of the precursor cluster **1** and possesses an η^5-cyclopentadienyl group, three bridging carbonyls arranged about a WIr_2 plane, six terminal carbonyl ligands, and two iridium-ligated triphenylphosphite ligands. The WIr_3 core distances ($W–Ir_{av} = 2.85$ Å, $Ir–Ir_{av} = 2.71$ Å) are slightly longer than those of **1** ($W–Ir_{av} = 2.82$ Å, $Ir–Ir_{av} = 2.699$ Å); core distances of the bis(phosphine)- or diphosphine-substituted complexes [CpWIr$_3$(μ-CO)$_3$(CO)$_6$(PPh$_3$)$_2$] [27], [CpWIr$_3$(μ-dppe)(μ-CO)$_3$(CO)$_6$] [26], [CpWIr$_3$(μ-dppm)(μ-CO)$_3$(CO)$_6$] [26] and [CpWIr$_3$(μ-dppa)(μ-CO)$_3$(CO)$_6$] [26] are also consistent with core expansion upon introduction of P-donor ligands. The shortest Ir–Ir bond in **6** [Ir(1)–Ir(2) 2.6941(5) Å] is between the phosphite-coordinated iridiums; a short Ir–Ir linkage between the phosphine-ligated iridiums is also seen in [CpWIr$_3$(μ-CO)$_3$(CO)$_6$(PPh$_3$)$_2$]. The cyclopentadienyl group is inclined towards the WIr_2 face containing the bridging carbonyl ligands. Ir–CO(terminal) interactions for **6** [1.830(9)–1.918(9) Å] and ∠Ir–C–O(terminal) [174.5(8)–180(1)°] are unexceptional. Carbonyls CO(1) and CO(48) bridge somewhat asymmetrically, both being displaced towards Ir(1) which bears the radially-ligated phosphite; it is possible that this asymmetry maximizes backbonding. The Ir–P distances [2.230(3), 2.239(3) Å] and intraphosphite bond lengths and angles are not unusual. The disposition of ligands in **6** is similar to that found previously in [CpWIr$_3$(μ-CO)$_3$(CO)$_6$(PPh$_3$)$_2$] [27]. Formal electron counting reveals that **6** has 60 e, electron precise for a tetrahedral cluster.

2.3. Discussion

As mentioned in Section 2.1, the IR spectra of **2**, **4**, **5** and **7** are indicative of the presence of isomers. The ^{31}P-NMR spectra of these clusters are also consistent with mixtures of isomers which interconvert on the NMR timescale. For example, the room temperature ^{31}P-NMR spectrum of **2** contains a broad resonance at 86.6 ppm. A low temperature limiting spectrum of two singlets (91.8 and 81.9 ppm, ratio 1:7) is obtained at 163 K. The variable temperature spectra of **2** (Fig. 3) reveal that these signals coalesce at 216 K (CS_2/CD_2Cl_2, 300 MHz). The room temperature ^{31}P-NMR spectra of complexes **4**, **5** and **7** contain a broadened weighted average resonance, or no signal at all. Lowering the temperature at which the spectra are obtained for each derivative sharpens the ^{31}P-NMR resonances, suggesting fluxionality in each case.

In analogous tetrairidium clusters Shapley has assigned down-field ^{31}P-NMR resonances to radially-coordinated phosphines and up-field signals to axially-coordinated phosphines [39]. This has been generalized and extended; in the ^{1}H-, ^{13}C- and ^{31}P-NMR

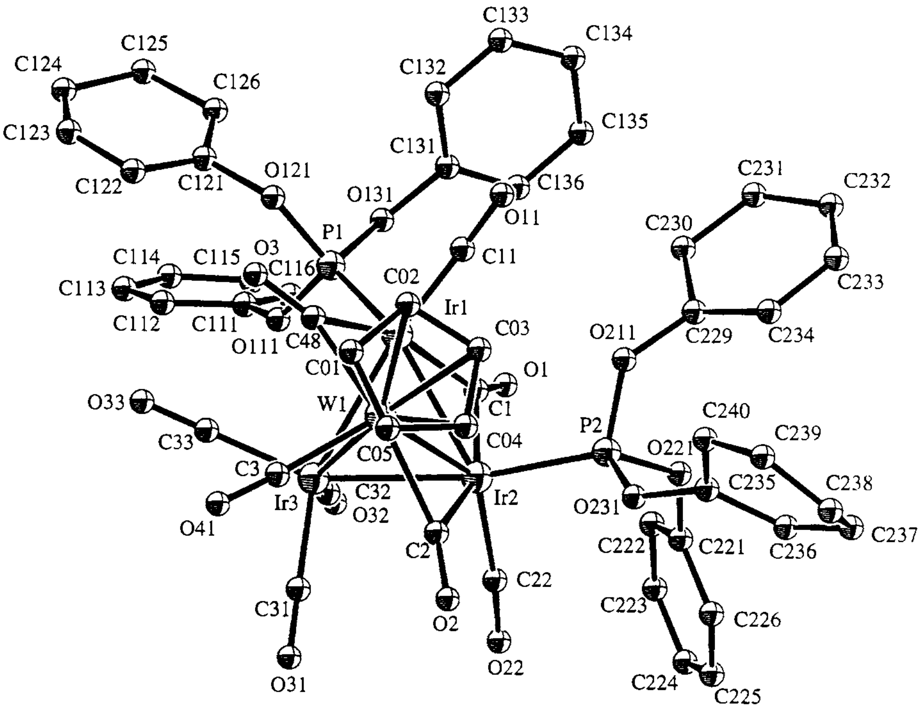

Fig. 2. Molecular structure and atomic labeling scheme for [CpWIr$_3$(μ-CO)$_3$(CO)$_6${P(OPh)$_3$}$_2$] (**6**). 20% thermal envelopes are shown for the non-hydrogen atoms; hydrogen atoms have arbitrary radii of 0.1 Å.

spectra of tetrairidium cluster compounds, the chemical shifts of the ligands decrease in the positional sequence: bridging > radial > axial ≈ apical [48]. Resonances of the phosphite-substituted tungsten–iridium clusters are listed in Table 3, together with suggested coordination geometries. The substitution sites have been assigned utilizing information from (a) the crystallographically-verified isomer, (b) the substitution geometries found in the analogous phosphine-substituted tungsten–iridium clusters and the tetrairidium system, and (c) chemical shifts in the ^{31}P-NMR spectra, assuming that the positional sequence is applicable to phosphite clusters.

Suggested geometries for the isomers of **5**–**7** are given in Fig. 4. The crystallographically observed cluster **6** has triphenylphosphite ligands occupying radial and axial sites and Cp occupying an axial site (radial, diaxial geometry). All structurally characterized tetrasubstituted tetrahedral tetrairidium clusters adopt radial, diaxial, apical geometries, with the apical ligand inclined to the bond between axial-ligated iridiums to minimize steric effects. Assuming that the predominant isomer of **7** in solution adopts this geometry, isomer **7a** has Cp occupying an axial site, and phosphites in radial, axial, apical sites (radial, diaxial, apical geometry). Utilizing the positional sequence of the ^{31}P-NMR shifts, the minor isomer of **7** is therefore of diradial, axial, apical geometry with the Cp in an apical site. The assignments of **6** and **7** permit discrimination of axially-ligated triphenylphosphite when Cp is in the basal plane (~ 60 ppm) or in an apical site (~ 80 ppm). The isomers of **5** may therefore be assigned. Isomer **5a** is assigned an axial phosphite, radial Cp geometry, and isomer **5b** an axial phosphite, apical Cp geometry; the latter geometry has been observed previously with a crystallographically characterized isomer of [CpWIr$_3$(μ-CO)$_3$(CO)$_7$(PMe$_3$)] [27]. Isomer **5c** is assigned a radial phosphite, axial Cp geometry, which has been observed previously with a crystallographically confirmed isomer of [CpWIr$_3$(μ-CO)$_3$(CO)$_7$(PPh$_3$)] [27].

Geometries of possible isomers of **2**–**4** are given in Fig. 5. The major isomer of **4** in solution is assigned a radial, diaxial, apical geometry with axial Cp, and the minor isomer a diradial, axial, apical geometry with apical Cp, both analogous to that observed with **7**. Cluster **3** is assigned a radial, diaxial geometry with axial Cp, analogous to that observed with the crystallographically characterized **6**. Replacing triphenylphosphite by trimethylphosphite in progressing for **6**, **7** to **3**, **4** results in a shift to low field of 15–20 ppm. Assuming that the same trend is observed in progressing from **5** to **2**, the observed isomers of **2** can be assigned radial Cp, axial phosphite (**2a**) and axial phosphite, apical Cp (**2b**) geometries, analogous to those observed with **5**.

It should be emphasized that these assignments are cautious, requiring a crystallographic underpinning to be solid. While many of these geometries have been structurally verified in the mixed-metal or parent tetrairidium systems, the diradial, axial, apical geometry is crystallographically unprecedented, and corroborating data is required to establish its existence. ^{31}P-NMR

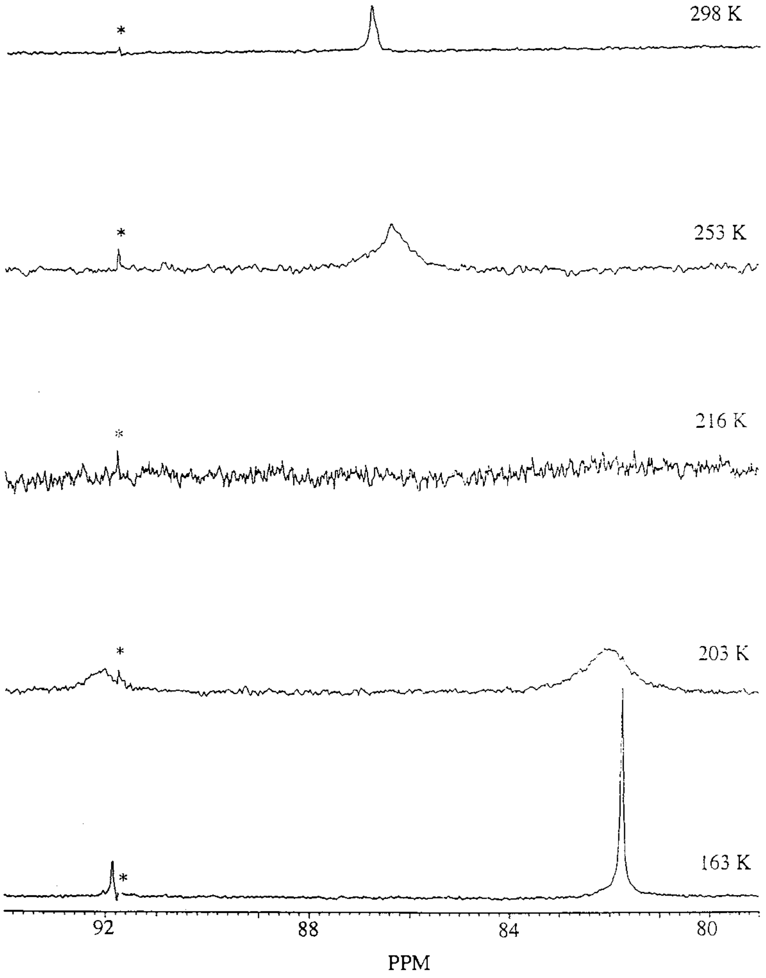

Fig. 3. Variable temperature ^{31}P-NMR spectra for **2**.

chemical shifts have been utilized to assign many of the geometries in the present work, but it is not certain that the positional sequence of chemical shifts radial > axial > apical consists of mutually exclusive chemical shift ranges; in particular instances, for example, it is possible that radial and axial shifts may be similar, rendering assignment speculative. With these caveats in mind, it has been possible to assign coordination geometries to all isomers observed in the phosphite system. Comparison to our earlier results with triphenylphosphine and trimethylphosphine reveals some differences. Unlike the bis-phosphite clusters, bis-phosphine clusters are observed as a mixture of two isomers, one of which has both phosphines in radial sites. The tris-trimethylphosphine derivative exists with a radial, diaxial, apical geometry (Cp axial) only, unlike the tris-phosphite clusters. The other geometries are observed in both phosphine and phosphite systems. Further studies probing the coordination geometries of ligand-substituted tetrahedral mixed-metal clusters are currently underway.

3. Experimental details

All reactions were performed under an atmosphere of dry nitrogen (high purity grade, CIG), although no special precautions were taken to exclude air during work-up. Dichloromethane was dried over CaH_2 under nitrogen prior to use; all other solvents were reagent grade, and used as received. Petroleum ether refers to a fraction of boiling point range 60–80°C. The products of TLC were separated on 20 × 20 cm glass plates coated with Merck GF_{254} silica gel. $[CpWIr_3(CO)_{11}]$ was prepared by the published procedure [54]. Trimethylphosphite (Aldrich) and triphenylphosphite (BDH) were purchased commercially and used as received.

Infrared spectra were recorded on a Perkin-Elmer System 2000 Fourier transform spectrophotometer using a 0.1 mm cell with CaF_2 windows. ^{1}H-NMR spectra were recorded on a Varian Gemini 300 spectrometer at 300 MHz. ^{31}P-NMR spectra were recorded on a Varian

Table 3
^{31}P-NMR data for [CpWIr$_3$(μ-CO)$_3$(CO)$_{8-n}$(L)$_n$] (L = P(OMe)$_3$, P(OPh)$_3$; n = 1, 2 or 3)

Complex		^{31}P-NMR shifts	Suggested site of phosphite substitution, with respect to (μ-CO)$_3$ plane	Suggested site of Cp substitution	Isomer ratio
$n = 1$, L = P(OMe)$_3$	**2a**	81.7[a]	Axial	Radial	7
	2b	91.8[a]	Axial	Apical	1
$n = 2$, L = P(OMe)$_3$	**3**	124.4, 83.8 (1:1)[b]	Radial, Axial	Axial	
$n = 3$, L = P(OMe)$_3$	**4a**	118.2, 97.1, 78.3 (1:1:1)[b]	Radial, Axial, Apical	Axial	2
	4b	118.5, 95.6 (2:1)[b]	Diradial, Axial	Apical	1
$n = 1$, L = P(OPh)$_3$	**5a**	64.8[a]	Axial	Radial	1
	5b	78.1[a]	Axial	Apical	2
	5c	103.2[a]	Radial	Axial	1
$n = 2$, L = P(OPh)$_3$	**6**	109.5, 65.9 (1:1)[b]	Radial, Axial[c]	Axial	
$n = 3$, L = P(OPh)$_3$	**7a**	107.7, 58.1, 35.2 (1:1:1)[b]	Radial, Axial, Apical	Axial	3
	7b	100.9, 78.8 (2:1)[b]	Diradial, Axial	Apical	1

[a] 4 CS$_2$/1 CD$_2$Cl$_2$, 163 K; [b] acetone-d_6, 230 K; [c] crystallographically confirmed.

VXR300S spectrometer at 121 MHz and are proton decoupled. Spectra were run in CDCl$_3$ (Aldrich), acetone-d_6 (Aldrich) or a 4:1 mixture of CS$_2$/CD$_2$Cl$_2$ (CS$_2$: Univar; CD$_2$Cl$_2$: Aldrich); chemical shifts in ppm are referenced to internal residual solvent for ^{1}H-NMR spectra and external 85% H$_3$PO$_4$ (0.0 ppm) for ^{31}P-NMR spectra.

Mass spectra were obtained at the Australian National University on a VG ZAB 2SEQ instrument (30 kV Cs$^+$ ions, current 1 mA, accelerating potential 8 kV, matrix 3-nitrobenzyl alcohol). Peaks were recorded as m/z based on ^{183}W assignments and are reported in the form: m/z (assignment, relative intensity). Elemental microanalyses were performed by the Microanalysis Service Unit in the Research School of Chemistry, Australian National University.

3.1. Reaction of [CpWIr$_3$(CO)$_{11}$] with one equivalent of P(OMe)$_3$

An orange solution of [CpWIr$_3$(CO)$_{11}$] (20.0 mg, 0.0176 mmol) and P(OMe)$_3$ (2.1 µl, 0.0175 mmol) in CH$_2$Cl$_2$ (20 ml) was stirred at room temperature for 18 h. The solution was then evaporated to dryness. The resultant orange residue was dissolved in CH$_2$Cl$_2$ (ca. 1 ml) and chromatographed (3 CH$_2$Cl$_2$:2 petroleum ether eluant). The contents of the first band were identified as [CpWIr$_3$(CO)$_{11}$] (1.5 mg, 7.5%) by solution IR spectroscopy. Crystallization of the contents of the second band, R$_f$ 0.42, from CH$_2$Cl$_2$/MeOH afforded orange crystals of [CpWIr$_3$(μ-CO)$_3$(CO)$_7${P(OMe)$_3$}], **2** (15.4 mg, 71%). **2**: IR (c-C$_6$H$_{12}$) 2078s, 2070w, 2060w, 2046vs, 2033m, 2022s, 2017vs, 1999m, 1995m, 1970m, 1959w, 1921m, 1841w, 1830w, 1825m, 1801w cm^{-1}; ^{1}H-NMR (CDCl$_3$) δ 4.98 (s, 5H, C$_5$H$_5$), 3.71 [d, J(HP) = 12 Hz, 9H, Me]; ^{31}P-NMR (CS$_2$/CD$_2$Cl$_2$, 188 K) δ 91.8 (s, 0.13P), 81.7 (s, 0.87P); MS 1230 ([M]$^+$, 15), 1202 ([M−CO]$^+$, 14), 1174 ([M−2CO]$^+$, 20), 1146 ([M−3CO]$^+$, 100), 1118 ([M−4CO]$^+$, 33) 1090 ([M−5CO]$^+$, 5). Anal. Calc.: C 17.58, H 1.15. Found: C 18.58, H 0.58%.

3.2. Reaction of [CpWIr$_3$(CO)$_{11}$] with two equivalents of P(OMe)$_3$

An orange solution of [CpWIr$_3$(CO)$_{11}$] (20.0 mg, 0.0176 mmol) and P(OMe)$_3$ (4.3 µl, 0.0352 mmol) in CH$_2$Cl$_2$ (20 ml) was stirred at room temperature for 18 h. The resultant dark orange solution was evaporated to dryness, the orange residue dissolved in CH$_2$Cl$_2$ (ca. 1 ml) and chromatographed (2 CH$_2$Cl$_2$:1 petroleum ether eluant) to afford two products, one of which was in trace amounts. The major product, R$_f$ 0.35, was crystallized from CH$_2$Cl$_2$/MeOH to afford orange crystals of [CpWIr$_3$(μ-CO)$_3$(CO)$_6${P(OMe)$_3$}$_2$], **3** (9.7 mg, 41%). **3**: IR (c-C$_6$H$_{12}$) 2065vs, 2042w, 2012vs, 1997m, 1983s, 1948m, 1910m, 1908w, 1819m cm^{-1}; ^{1}H-NMR (CDCl$_3$) δ 4.93 (s, 5H, C$_5$H$_5$), 3.73 [d, J(HP) = 12 Hz, 18H, Me]; ^{31}P-NMR (acetone-d_6, 230 K) δ 124.4 (s, 1P), 83.8 (s, 1P); MS 1270 ([M−2CO]$^+$, 20), 1242 ([M−3CO]$^+$, 100), 1214 ([M−4CO]$^+$, 20), 1186 ([M−5CO]$^+$, 17). Anal. Calc.: C 18.12, H 1.75. Found: C 18.23, H 1.40%.

3.3. Reaction of [CpWIr$_3$(CO)$_{11}$] with three equivalents of P(OMe)$_3$

An orange solution of [CpWIr$_3$(CO)$_{11}$] (20.0 mg, 0.0176 mmol) and P(OMe)$_3$ (10 µl, 0.083 mmol) in

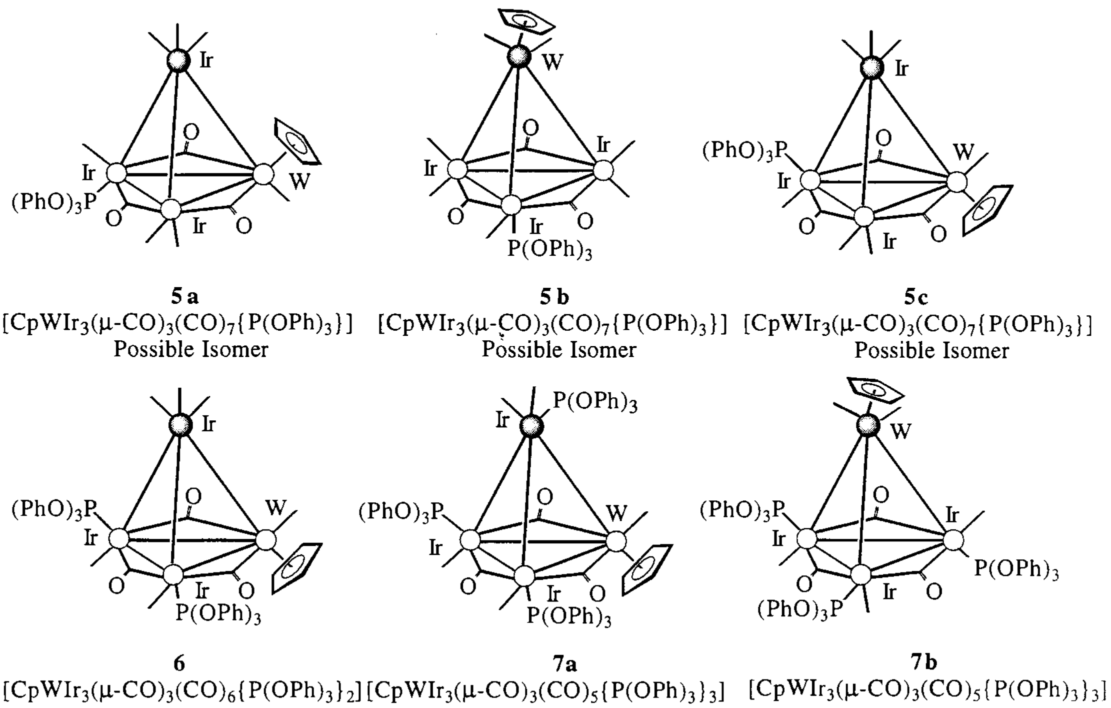

5a [CpWIr$_3$(μ-CO)$_3$(CO)$_7${P(OPh)$_3$}] Possible Isomer

5b [CpWIr$_3$(μ-CO)$_3$(CO)$_7${P(OPh)$_3$}] Possible Isomer

5c [CpWIr$_3$(μ-CO)$_3$(CO)$_7${P(OPh)$_3$}] Possible Isomer

6 [CpWIr$_3$(μ-CO)$_3$(CO)$_6${P(OPh)$_3$}$_2$]

7a [CpWIr$_3$(μ-CO)$_3$(CO)$_5${P(OPh)$_3$}$_3$]

7b [CpWIr$_3$(μ-CO)$_3$(CO)$_5${P(OPh)$_3$}$_3$]

Fig. 4. Possible configurations for [CpWIr$_3$(μ-CO)$_3$(CO)$_{8-n}${P(OPh)$_3$}$_n$] (**5**–**7**).

CH_2Cl_2 (20 ml) was refluxed for 3 h. The resultant dark orange solution was evaporated to dryness, the orange residue dissolved in CH_2Cl_2 (ca. 1 ml) and chromatographed (2 CH_2Cl_2:1 petroleum ether eluant) to afford three products. The contents of the first two bands were characterized as **2** and **3** by IR spectroscopy. The third band, R_f 0.16, was crystallized from CH_2Cl_2/MeOH to afford orange crystals of [CpWIr$_3$(μ-CO)$_3$(CO)$_5${P(OMe)$_3$}$_3$], **4** (7.2 mg, 29%). **4**: IR (c-C_6H_{12}) 2008s, 1992vs, 1974s, 1940m, 1908w, 1901m, 1898w, 1844w, 1802m cm^{-1}; ^{1}H-NMR ($CDCl_3$) δ 4.71 [s (br), 5H, C_5H_5], 3.91–3.78 (m, 27H, Me); ^{31}P-NMR (acetone-d_6, 230 K) δ 118.2 (s, 0.67P), 97.1 (s, 0.67P), 78.3 (s, 0.67P); 118.5 (s, 0.67P), 95.6 (s, 0.33P); MS 1338 ([M−3CO]$^+$, 100), 1310 ([M−4CO]$^+$, 11), 1282 ([M−5CO]$^+$, 8), 1254 ([M−6CO]$^+$, 35). Anal. Calc.: C 18.58, H 2.27. Found: C 18.90, H 1.91%.

3.4. Reaction of [CpWIr$_3$(CO)$_{11}$] with one equivalent of P(OPh)$_3$

An orange solution of [CpWIr$_3$(CO)$_{11}$] (20.1 mg, 0.0177 mmol) and P(OPh)$_3$ (4.6 μl, 0.0177 mmol) in CH_2Cl_2 (20 ml) was stirred at room temperature for 24 h. The solution was then evaporated to dryness. The resultant orange residue was dissolved in CH_2Cl_2 (ca. 1 ml) and chromatographed (3 CH_2Cl_2:2 petroleum ether eluant), two bands being identified. The contents of the first band were found to be **1** by IR spectroscopy. Crystallization of the contents of the second band, R_f 0.51, from CH_2Cl_2/MeOH afforded orange crystals of [CpWIr$_3$(μ-CO)$_3$(CO)$_7${P(OPh)$_3$}], **5** (11.2 mg, 45%). **5**: IR (c-C_6H_{12}) 2080vs, 2071w, 2047vs, 2029vs, 2020s, 2008m, 1997m, 1967m, 1927w, 1925br w, 1854w, 1825w, 1802w cm^{-1}; ^{1}H-NMR (acetone-d_6) δ 8.02 (s, 0.66H, $CHCl_3$), 7.33–7.02 (m, 15H, OPh), 5.04 (s, 5H, C_5H_5); ^{31}P-NMR (CS_2/CD_2Cl_2, 188 K) δ 103.2 (s, 0.25P), 78.1 (s, 0.50P), 64.8 (s, 0.25P); MS 1416 ([M]$^+$, 5), 1388 ([M−CO]$^+$, 7), 1360 ([M−2CO]$^+$, 12), 1332 ([M−3CO]$^+$, 15), 1304 ([M−4CO]$^+$, 13), 1276 ([M−5CO]$^+$, 100), 1248 ([M−6CO]$^+$, 35), 1220 ([M−7CO]$^+$, 14), 1192 ([M−8CO]$^+$, 57), 1164 ([M−9CO]$^+$, 34), 1136 ([M−10CO]$^+$, 27). Anal. Calc.: C 27.04, H 139. Found: C 27.08, H 1.42%.

3.5. Reaction of [CpWIr$_3$(CO)$_{11}$] with two equivalents of P(OPh)$_3$

An orange solution of [CpWIr$_3$(CO)$_{11}$] (20.2 mg, 0.0178 mmol) and P(OPh)$_3$ (9.3 μl, 0.0356 mmol) in CH_2Cl_2 (20 ml) was stirred at room temperature for 24 h. The dark orange solution was evaporated to dryness. The resultant orange residue was dissolved in CH_2Cl_2 (ca. 1 ml) and chromatographed (2 CH_2Cl_2:1 petroleum ether eluant) to afford two products, one of which was in trace amounts. The major product, R_f 0.35, was crystallized from CH_2Cl_2/MeOH to afford orange crystals of [CpWIr$_3$(μ-CO)$_3$(CO)$_6${P(OPh)$_3$}$_2$], **6** (12.3 mg, 41%). **6**: IR (c-C_6H_{12}) 2069vs, 2045w, 2021vs, 2008s, 1987m, 1957m, 1917m, 1906m, 1830w cm^{-1}; ^{1}H-NMR ($CDCl_3$) δ 7.30–7.00 (m, 30H, OPh), 4.99 (s, 5H,

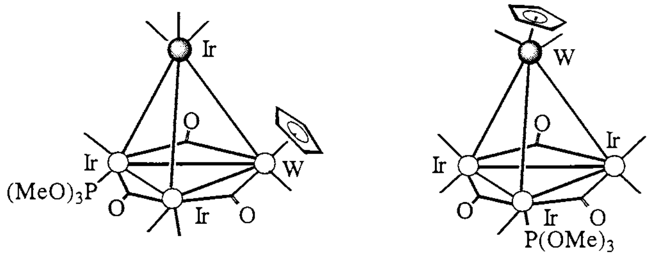

2a $[CpWIr_3(\mu\text{-}CO)_3(CO)_7\{P(OMe)_3\}]$ Possible isomer

2b $[CpWIr_3(\mu\text{-}CO)_3(CO)_7\{P(OMe)_3\}]$ Possible isomer

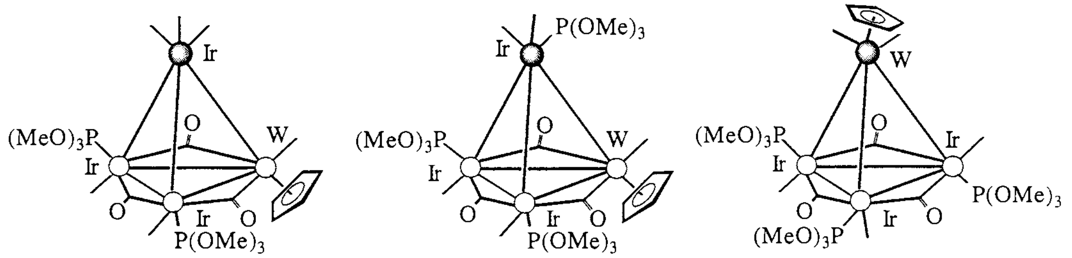

3 $[CpWIr_3(\mu\text{-}CO)_3(CO)_6\{P(OMe)_3\}_2]$ **4a** $[CpWIr_3(\mu\text{-}CO)_3(CO)_5\{P(OMe)_3\}_3]$ **4b** $[CpWIr_3(\mu\text{-}CO)_3(CO)_5\{P(OMe)_3\}_3]$

Fig. 5. Possible configurations for $[CpWIr_3(\mu\text{-}CO)_3(CO)_{8-n}\{P(OMe)_3\}_n]$ (**2**–**4**).

C_5H_5); ^{31}P-NMR (acetone-d_6, 230 K) δ 109.5 (s, 1P), 65.9 (s, 1P); MS 1558 ([M−5CO]$^+$, 68), 1530 ([M−6CO]$^+$, 28), 1502 ([M−7CO]$^+$, 75), 1474 ([M−8CO]$^+$, 100), 1446 ([M−9CO]$^+$, 64). Anal. Calc.: C 35.36, H 2.08. Found: C 35.95, H 1.83%. A crystal suitable for the X-ray diffraction study was grown by slow diffusion of hexane into dichloromethane at −5°C.

3.6. Reaction of $[CpWIr_3(CO)_{11}]$ with three equivalents of $P(OPh)_3$

An orange solution of $[CpWIr_3(CO)_{11}]$ (20.2 mg, 0.0178 mmol) and $P(OMe)_3$ (23.3 µl, 0.089 mmol) in CH_2Cl_2 (20 ml) was refluxed for 3 h. The dark orange solution obtained was evaporated to dryness. The resultant orange residue was dissolved in CH_2Cl_2 (ca. 1 ml) and chromatographed (2 CH_2Cl_2:1 petroleum ether eluant) to afford two products, the contents of the first band being characterized as **6** by IR spectroscopy. The third band, R_f 0.18, was crystallized from CH_2Cl_2/MeOH to afford orange crystals of $[CpWIr_3(\mu\text{-}CO)_3(CO)_5\{P(OMe)_3\}_3]$, **7** (11.2 mg, 32%). **7**: IR (c-C_6H_{12}) 2069s, 2043m, 2021s, 2013vs, 1989m, 1954m, 1912m, 1909m, 1843br w cm^{-1}; ^{1}H-NMR ($CDCl_3$) δ 7.31–7.01 (m, 45H, Ph), 4.97 [s (br), 5H, C_5H_5]; ^{31}P-NMR (acetone-d_6, 230 K) δ 107.7 (s, 0.75P), 58.1 (s, 0.75P), 35.2 (s, 0.75P); 100.9 (s, 0.50P), 78.8 (s, 0.25P); MS 1896 ([M−3CO]$^+$, 41), 1868 ([M−4CO]$^+$, 6), 1840 ([M−5CO]$^+$, 10), 1812 ([M−6CO]$^+$, 11), 1784 ([M−7CO]$^+$, 20). Satisfactory analyses could not be obtained due to sample decomposition over days.

3.7. Structure determination

Crystals of compound **6** suitable for diffraction analysis were grown by slow diffusion of hexane into dichloromethane at −5°C. A unique diffractometer data set was measured at ~295 K within the specified $2\theta_{max}$ limit ($2\theta/\theta$ scan mode; monochromatic Mo-Kα radiation ($\lambda = 0.7107_3$ Å)) yielding N independent reflections. N_o of these with $I > 3\sigma(I)$ were considered 'observed' and used in the full matrix/large block least squares refinements after analytical absorption correction. Anisotropic thermal parameters were refined for the non-hydrogen atoms; $(x, y, z, U_{iso})_H$ were included, constrained at estimated values. High thermal motion in the phenyl rings is indicative of disorder which could not be resolved into separate components; as a result, one of the rings is buckled. Conventional residuals R, R_w on $|F|$ at convergence are given. Neutral atom complex scattering factors were used, computation using teXsan [55]. Pertinent results are given in the figures and tables. Atomic coordinates, bond lengths and angles, and thermal parameters have been deposited at the Cambridge Structural Database.

Acknowledgements

We thank the Australian Research Council for support of this work and Johnson-Matthey Technology Center for the generous loan of $IrCl_3$. MGH is an ARC Australian Research Fellow.

References

[1] N.T. Lucas, M.G. Humphrey, M.L. Williams, P.C. Healy, J. Organomet. Chem. 545–546 (1997) 519.

[2] W.L. Gladfelter, J.R. Fox, J.A. Smegal, T.G. Wood, G.L. Geoffroy, Inorg. Chem. 20 (1981) 3223.

[3] M.I. Bruce, J. Organomet. Chem. 242 (1983) 147.

[4] M.I. Bruce, J. Organomet. Chem. 17 (1985) 399.

[5] E. Sappa, A. Tiripicchio, P. Braunstein, Coord. Chem. Rev. 65 (1985) 219.

[6] E.W. Abel, F.G.A. Stone, G. Wilkinson (Eds.), Comprehensive Organometallic Chemistry II, vol. 10, Pergamon, Oxford, UK, 1995.

[7] W.E. Lindsell, N.M. Walker, A.S.F. Boyd, J. Chem. Soc. Dalton Trans. (1988) 675.

[8] J. Pursiainen, M. Ahlgren, T. Pakkanen, J. Valkonen, J. Chem. Soc. Dalton Trans. (1990) 1147.

[9] O.J. Curnow, J.W. Kampf, M.D. Curtis, Organometallics 10 (1991) 2546.

[10] I. Ojima, R.J. Donovan, N. Clos, Organometallics 10 (1991) 2606.

[11] J.-L. Le Grand, W.E. Lindsall, K.J. McCullough, J. Organomet. Chem. 413 (1991) 321.

[12] J.-L. Le Grand, W.E. Lindsall, K.J. McCullough, C.H. McIntosh, A.G. Meiklejohn, J. Chem. Soc. Dalton Trans. (1992) 1089.

[13] J.R. Fox, W.L. Gladfelter, T.G. Wood, J.A. Smegal, T.K. Foreman, G.L. Geoffroy, I. Tavanaiepour, V.W. Day, C.S. Day, Inorg. Chem. 20 (1981) 3214.

[14] I.T. Horvath, Organometallics 5 (1986) 2333.

[15] E. Sappa, M.L.N. Marchino, G. Predieri, A. Tiripicchio, M.T. Camellini, J. Organomet. Chem. 307 (1986) 97.

[16] M. Bojczuk, B.T. Heaton, S. Johnson, C.A. Ghilardi, A. Orlandini, J. Organomet. Chem. 341 (1988) 473.

[17] T.A. Pakkanen, J. Pursianen, T. Venäläinen, T.T. Pakkanen, J. Organomet. Chem. 372 (1989) 129.

[18] J. Pursianen, T.A. Pakkanen, Acta Chem. Scand. Ser. A 43 (1989) 463.

[19] H. Matsuzaka, T. Kodama, Y. Uchida, M. Hidai, Organometallics 7 (1988) 1608.

[20] J. Pursiainen, T.A. Pakkanen, J. Jääskeläinen, J. Organomet. Chem. 290 (1985) 85.

[21] A.A. Bahsoun, J.A. Osborn, C. Voelker, J.J. Bonnet, G. Lavigne, Organometallics 1 (1982) 1114.

[22] H. Eshtiagh-Hosseini, J.F. Nixon, J. Organomet. Chem. 150 (1978) 129.

[23] D. Labroue, R. Queau, R. Poilblanc, J. Organomet. Chem. 186 (1980) 101.

[24] B.T. Huie, C.B. Knobler, H.D. Kaesz, J. Am. Chem. Soc. 100 (1978) 3059.

[25] J.-L. Le Grand, W.E. Lindsall, K.J. McCullough, J. Organomet. Chem. 373 (1989) C1.

[26] J. Lee, M.G. Humphrey, D.C.R. Hockless, B.W. Skelton, A.H. White, Organometalllics 12 (1993) 3468.

[27] S.M. Waterman, M.G. Humphrey, V.-A. Tolhurst, B.W. Skelton, A.H. White, Organometallics 15 (1996) 934.

[28] S.M. Waterman, M.G. Humphrey, V.-A. Tolhurst, B.W. Skelton, A.H. White, J. Organomet. Chem. 507 (1995) 163.

[29] S.M. Waterman, M.G. Humphrey, D.C.R. Hockless, Organometallics 15 (1995) 1745.

[30] N.T. Lucas, M.G. Humphrey, D.C.R. Hockless, J. Organomet. Chem. 535 (1997) 175.

[31] N.T. Lucas, I.R. Whittall, M.G. Humphrey, D.C.R. Hockless, M.P.S. Perera, M.L. Williams, J. Organomet Chem. 540 (1997) 147.

[32] E. Band, E.L. Muetterties, Chem. Rev. 78 (1978) 639.

[33] B.E. Mann, Ann. Rep. NMR Spectroscopy 12 (1982) 263.

[34] K. Orrell, V. Sik, Ann. Rep. NMR Spectroscopy 19 (1987) 79.

[35] K. Orrell, V. Sik, Ann. Rep. NMR Spectroscopy 27 (1993) 103.

[36] V. Albano, P. Bellon, V. Scatturin, Chem. Commun. (1967) 730.

[37] A.J. Drakesmith, R. Whyman, J. Chem. Soc. Dalton Trans. (1973) 362.

[38] K.J. Karel, J.R. Norton, J. Am. Chem. Soc. 96 (1974) 6812.

[39] G.F. Stuntz, J.R. Shapley, Inorg. Chem. 15 (1976) 1994.

[40] G.F. Stuntz, J.R. Shapley, J. Am. Chem. Soc. 99 (1977) 607.

[41] F. Demartin, M. Manassero, M. Sansoni, L. Garlaschelli, U. Sartorelli, J. Organomet. Chem. 204 (1981) C10.

[42] D.J. Darensbourg, B.J. Baldwin-Zuschke, Inorg. Chem. 20 (1982) 3846.

[43] B.E. Mann, C.M. Spencer, A.K. Smith, J. Organomet. Chem. 244 (1983) C17.

[44] A.J. Blake, A.G. Osborne, J. Organomet. Chem. 260 (1984) 227.

[45] M.M. Harding, B.S. Nicholls, A.K. Smith, Acta Crystallogr. C40 (1984) 790.

[46] J.A. Clucas, M.M. Harding, B.S. Nicholls, A.K. Smith, J. Chem. Soc. Chem. Commun. (1984) 319.

[47] V.G. Albano, D. Braga, R. Ros, A. Scrivanti, J. Chem. Soc. Chem. Commun. (1985) 866.

[48] R. Ros, A. Scrivanti, V.G. Albano, D. Braga, J. Chem. Soc. Dalton Trans. (1986) 2411.

[49] D. Braga, F. Grepioni, G. Guadalupi, A. Scrivanti, R. Ros, R. Roulet, Organometallics 6 (1987) 56.

[50] A. Strawczynski, R. Ros, R. Roulet, D. Braga, C. Gradella, F. Grepioni, Inorg. Chim. Acta 170 (1990) 17.

[51] A. Strawczynski, C. Hall, G. Bondietti, R. Ros, R. Roulet, Helv. Chim. Acta 77 (1994) 754.

[52] G. Laurenczy, G. Bondietti, R. Ros, R. Roulet, Inorg. Chim. Acta 247 (1996) 65.

[53] K. Besancon, G. Laurenczy, T. Lumini, R. Roulet, Helv. Chim. Acta 76 (1993) 2926.

[54] J.R. Shapley, S.J. Hardwick, D.S. Foose, G.D. Stucky, J. Am. Chem. Soc. 103 (1981) 7383.

[55] teXsan: Single Crystal Structure Analysis Software, version 1.7-3, Molecular Structure Corporation, The Woodlands, TX, USA, 1995.